Molecules and Cells

Enhancer Function of MicroRNA-3681 Derived from Long Terminal Repeats Represses the Activity of Variable Number Tandem Repeats in the 3' UTR of *SHISA7*

Hee-Eun Lee[1,2,3], Sang-Je Park[3], Jae-Won Huh[3,4], Hiroo Imai[5], and Heui-Soo Kim[2,6,*]

[1]Department of Integrated Biological Science, Pusan National University, Busan 46241, Korea, [2]Institute of Systems Biology, Pusan National University, Busan 46241, Korea, [3]National Primate Research Center, Korea Research Institute of Bioscience and Biotechnology, Cheongju 28116, Korea, [4]Department of Functional Genomics, Korea Research Institute of Bioscience and Biotechnology (KRIBB) School of Bioscience, Korea University of Science and Technology (UST), Daejeon 34113, Korea, [5]Department of Cellular and Molecular Biology, Primate Research Institute, Kyoto University, Inuyama 484-8506, Japan, [6]Department of Biological Sciences, College of Natural Sciences, Pusan National University, Busan 46241, Korea
*Correspondence: khs307@pusan.ac.kr
https://doi.org/10.14348/molcells.2020.0058
www.molcells.org

microRNAs (miRNAs) are non-coding RNA molecules involved in the regulation of gene expression. miRNAs inhibit gene expression by binding to the 3′ untranslated region (UTR) of their target gene. miRNAs can originate from transposable elements (TEs), which comprise approximately half of the eukaryotic genome and one type of TE, called the long terminal repeat (LTR) is found in class of retrotransposons. Amongst the miRNAs derived from LTR, hsa-miR-3681 was chosen and analyzed using bioinformatics tools and experimental analysis. Studies on hsa-miR-3681 have been scarce and this study provides the relative expression analysis of hsa-miR-3681-5p from humans, chimpanzees, crab-eating monkeys, and mice. Luciferase assay for hsa-miR-3681-5p and its target gene *SHISA7* supports our hypothesis that the number of miRNA binding sites affects target gene expression. Especially, the variable number tandem repeat (VNTR) and hsa-miR-3681-5p share the binding sites in the 3' UTR of *SHISA7*, which leads the enhancer function of hsa-miR-3681-5p to inhibit the activity of VNTR. In conclusion, hsa-miR-3681-5p acts as a super-enhancer and the enhancer function of hsa-miR-3681-5p acts as a repressor of VNTR activity in the 3′ UTR of *SHISA7*.

Keywords: long terminal repeat, miR-3681-5p, *SHISA7*, transposable elements, variable number tandem repeat

INTRODUCTION

Transposable elements (TEs) comprise approximately half of the eukaryotic genome and are known to insert into the genome as stable genomic components (Bourque et al., 2018; Wicker et al., 2007). TEs are divided into two classes—retrotransposons (class I) and DNA transposons (class II). Retrotransposons use the 'copy and paste' mechanism. The retrotransposons are first transcribed into an RNA intermediate, which is reverse transcribed into a DNA intermediate (Agren and Clark, 2018; Bourque et al., 2018; Lander et al., 2001; Wicker et al., 2007). Long terminal repeat (LTR) is a member of the retrotransposon family and the composition of LTR

Received 4 March, 2020; revised 12 May, 2020; accepted 27 May, 2020; published online 10 July, 2020

eISSN: 0219-1032

in humans is approximately 9%. An LTR consists of innate enhancer activity, however, transcription factor (TF), nucleotide substitutions, transcription start sites, and epigenetics may provide alternative enhancer activity of LTR elements (Thompson et al., 2016). LTRs recruit TF and enhance the transcription of host genes (Gonzalez-Cao et al., 2016; Hu et al., 2017). TEs can generate regulators of genes, such as microRNAs (miRNAs), TFs, and variable number tandem repeats (VNTRs) (Feschotte, 2008; Lee et al., 2019; Piriyapongsa et al., 2007; Qin et al., 2015; Roberts et al., 2014; Sabino et al., 2014).

miRNAs are small non-coding RNA molecules, approximately 19 to 24 nucleotides long, which are essential for gene regulation (Ambros et al., 2003; Bartel, 2004; Kim, 2005; O'Brien et al., 2018). miRNAs have a unique seed region, approximately six nucleotides long, that binds to the 3′ untranslated region (UTR) of the target mRNA. In most of cases, miRNAs regulate gene expression by inhibiting gene expression; however, recent study has reported the presence of enhancer miRNAs (Lee et al., 2019). In addition, some miRNAs bind to the 5′ UTR of the target transcripts and to coding sequences, to regulate target gene expression (Brummer and Hausser, 2014; Gu et al., 2014; Hausser et al., 2013; Lee et al., 2009; Li et al., 2016; Liu et al., 2015). In studies on miRNA, the number of miRNA binding sites in the target gene was not an important consideration in selecting the best target genes. Previous studies have suggested that miRNAs derived from transposable element (MDTE) and MDTEs share sequences (Lee et al., 2019; Petri et al., 2019; Piriyapongsa and Jordan, 2007; Piriyapongsa et al., 2007; Qin et al., 2015; Roberts et al., 2014). Hsa-miR-3681 is derived from an LTR element and has not been studied much. A few studies on hsa-miR-3681 have reported on its dysregulation in human disease and cancer and downregulation in cervical cancer (Shi et al., 2019; Vaira et al., 2014; Vaz et al., 2010).

One of target genes for hsa-miR-3681-5p, *SHISA7*, is a regulator of long-term synaptic potentiation, and plays an important role in regulating the neurotransmitter of gamma-aminobutyric acid (Han et al., 2019). A few reports have predicted that *SHISA7* is an miRNAs target and one study has reported that miRNA downregulates *SHISA7* expression in neuroblastoma cells (Cai et al., 2018; Marques et al., 2012; Yamamura et al., 2018). The 3′ UTR of *SHISA7* includes VNTRs, which are organized into 10 to 100 bp tandem repeats and often shows variations in the number of repeats among individuals (Nakamura et al., 1987). Previous reports have suggested that the VNTR in the 3′ UTR of the human dopamine transporter (*DAT*) regulates the expression of *DAT* (Inoue-Murayama et al., 2002). Another study has shown that the 3′ UTR can act as a regulator and enhancer to induce transcription (Jash et al., 2012).

In this study, the relative expression of the MDTEs, hsa-miR-3681-5p and its target *SHISA7*, was profiled in human, chimpanzee, crab-eating monkey, and mouse to compare its relative expression in evolutionary terms. Another aim of this study was to evaluate the impact of the number of miRNA binding sites on the regulation of target gene expression. In addition, the role of VNTR, with conserved hsa-miR-3681-5p seed region, in the 3′ UTR of *SHISA7* is discussed for further studies.

MATERIALS AND METHODS

Ethical statement

Experiments with the Western chimpanzee were carried out in accordance with the guidelines and regulations approved by the Animal Experimentation Committees of Kyoto University (2018-004). Experiments with Crab-eating monkey were carried out in accordance with guidelines and regulation approved by Korea Research Institute of Bioscience & Biotechnology (KRIBB-AEC-15046).

Bioinformatic analyses

The sequence of hsa-miR-3681-5p was downloaded from miRbase v22.1 (http://www.mirbase.org) (Kozomara et al., 2019), and then the sequence was used to localized in human genome (GRCh38) and to download sequence of LTR16D1 by UCSC Genome Browser (http://genome.ucsc.edu) (Agarwal et al., 2015). The sequences of hsa-miR-3681-5p and LTR16D1 were aligned using BioEdit (http://www.mbio.ncsu.edu/BioEdit/bioedit.html) (Hall, 1999) to compare the analogy. TargetScanHuman (http://www.targetscan.org/vert_72/) (Agarwal et al., 2015) was used to list out the target gene candidates of hsa-miR-3681-5p (Table 1).

The structural interaction between hsa-miR-3681-5p and the 3′ UTR of *SHISA7* was generated using BiBiServ RNAhybrid (https://bibiserv.cebitec.uni-bielefeld.de/rnahybrid) (Rehmsmeier et al., 2004). BiBiServ RNAhybrid is used to predict target genes and analyze the minimum free energy values, which represent the score of binding affinity between the miRNA and the target gene. The sequences of *SHISA7* and hsa-miR-3681-5p were used to detect complementary binding sites of hsa-miR-3681-5p in the 3′ UTR of *SHISA7*. Primers were designed using Primer3 v 4.1 (http://primer3.ut.ee/) (Koressaar et al., 2018) (Table 2).

The putative TF binding sites near the 9.5 VNTRs of the 3′ UTR of *SHISA7* was predicted using MATCH in TRANSFAC v8.0 (http://www.gene-regulation.com) (Kel et al., 2003; Wingender et al., 2001). Threshold values greater than 0.98 in both core match and matrix match were used for the prediction. Matrix match indicates the quality of the match between a matrix and a random part of the input sequence. Core match determines the quality of a match between the core sequences of a matrix.

Human and animal samples

Total RNAs from 13 human tissues (brain, heart, lung, liver, kidney, spleen, stomach, small intestine, colon, muscle, testis, prostate, and uterus) and 10 mouse tissues (brain, heart, lung, liver, kidney, spleen, stomach, smooth muscle, testis, and spinal cord) were purchased from Clontech (USA).

A total of 14 female crab-eating monkey tissue samples (cerebellum, cerebrum, heart, lung, liver, kidney, spleen, stomach, small intestine, large intestine, uterus, pancreas, bladder, and spinal cord) were provided by the National Primate Research Center (Korea). Total RNA was extracted from 14 tissue samples of the female crab-eating monkey by using Hybrid-R™ (GeneAll, Korea), according to the manufacturer's

Table 1. The list of target gene candidates of hsa-miR-3681-5p

Gene name	Abbreviation	Coordinates	Transcript ID	Total sites	8mer	7mer-m8	7mer-A1	6mer
Shisa family member 7	**SHISA7**	**chr19:55,428,738 -55,442,863**	**ENST00000376325.4**	**12**	**8**	**2**	**2**	**3**
ADP-ribosylation factor-like 10	ARL10	chr5:176,365,373 -176,381,963	ENST00000310389.5	4	0	2	2	2
Solute carrier family 8 (sodium/calcium exchanger), member 2	SLC8A2	chr19:47,428,017 -47,471,893	ENST00000236877.6	7	0	0	7	4
Myopalladin	MYPN	chr10:68,105,215 -68,211,985	ENST00000358913.5	4	1	1	2	1
Zinc finger and BTB domain containing 37	ZBTB37	chr1:173,868,082 -173,903,547	ENST00000367701.5	4	0	4	0	2
K(lysine) acetyltransferase 7	KAT7	chr17:49,788,681 -49,835,026	ENST00000259021.4	4	0	2	2	5
Glutamate receptor, ionotropic, N-methyl D-aspartate 2B	GRIN2B	chr12:13,537,337 -13,980,356	ENST00000609686.1	5	2	1	2	5
Lysine (K)-specific demethylase 5A	KDM5A	chr12:280,057 -389,320	ENST00000399788.2	5	0	3	2	4
RNA binding motif protein 28	RBM28	chr7:128,297,685 -128,343,908	ENST00000223073.2	4	1	1	2	4
Neuronal growth regulator 1	NEGR1	chr1:71,395,943 -72,282,539	ENST00000357731.5	4	1	2	1	4
Zinc finger and BTB domain containing 20	ZBTB20	chr3:114,304,949 -115,155,228	ENST00000462705.1	4	0	3	1	3
Peroxisomal biogenesis factor 26	PEX26	chr22:18,077,990 -18,105,396	ENST00000329627.7	4	1	3	0	0
Peptidylprolyl isomerase (cyclophilin)-like 4	PPIL4	chr6:149,504,495 -149,546,043	ENST00000340881.2	4	0	3	1	3

SHISA7, shown in bold, was selected as the hsa-miR-3681-5p target gene. Each column shows the name of the target gene, abbreviation of the gene name, the coordinates in the human chromosome, transcript ID, total hsa-miR-3681-5p binding sites in the 3′ UTR, number of binding sites for 8-mer, number of binding sites for 7-mer-m8, number of binding sites for 7-mer-A1, and number of binding sites for 6-mer.

Table 2. The list of primer information on SHISA7 and the reference gene

Primer	Sequences	Temperature (°C)	Details
9mer1	F: CATCTCCAGGGATCCACTTC R: GACACCAGGGTTATGGTGGA	55	One 9mer hsa-miR-3681-5p in 3' UTR of *SHISA7*
9mer3	F: AGGATCCACGAGAGCCAAT R: ATGGTGACAGACAGCACTGG	59	Three 9mer hsa-miR-3681-5p in 3' UTR of *SHISA7*
9mer6	F: CACTACCTCCCAGTATCCA R: ATGGTTGCAGTGGACTCT	55	Six 9mer hsa-miR-3681-5p in 3' UTR of *SHISA7*
G3PDH	F: GAA ATC CCA TCA CCA TCT TCC AGG R: GAG CCC CAG CCT TCT CCA TG	55	The reference gene; Glyceraldehyde 3-phosphate dehydrogenase (*G3PDH*)

Each primer was designed based on the quantity of 9mer hsa-miR-3681-5p binding sites. The name of the primer, sequence of each forward (F) and reverse (R) primer, annealing temperature and details about the primer is shown in the table.

instructions.

Tissue samples from the female Western chimpanzee were provided from the Kumamoto sanctuary, Kyoto University, to Primate Research Institute in Inuyama, Japan, via GAIN and the male Western chimpanzee samples were provided by the Primate Research Institute. All experiments using samples from the Western chimpanzee were done at the Primate Research Institute. Total RNA was extracted from 11 tissues of healthy male Western chimpanzees (cerebellum, heart, lung, liver, kidney, spleen, stomach, small intestine, colon, muscle, and testis) and female Western chimpanzees (cerebellum, heart, lung, liver, kidney, spleen, stomach, small intestine, colon, muscle, and ovary) by using Hybrid-R™, according to the manufacturer's instructions.

The RNA samples were quantitated using the ND-1000 UV-Vis spectrophotometer (NanoDrop, USA). A total of 500 ng of quantified RNA was reverse transcribed from mRNA by using PrimeScript RT Reagent Kit with gDNA Eraser (TaKaRa, Japan) and from miRNA by using HB miR Multi Assay Kit™ system I (HeimBiotek, Korea).

Quantitative polymerase chain reaction amplification

The quantitative polymerase chain reaction (qPCR) primer information for *SHISA7* and the reference gene is listed in Table 2. cDNA samples from humans, male and female Western chimpanzees, female crab-eating monkeys, and male mice were used with the SYBR Green Q-PCR Master Mix with High Rox (SmartGene, Korea) for qPCR, according to the manufacturer's instructions in a Rotor-Gene Q system (Qiagen, Germany), under the following qPCR conditions; initialization step at 95°C for 2 min, followed by 45 thermal cycles of 95°C for 5 s, 55°C for 10 s, and 72°C for 15 s; standard melting conditions of the ramp ranged from 55°C to 99°C, with a 1°C rise at each step. Glyceraldehyde 3-phosphate dehydrogenase (*G3PDH*) was used as the reference gene for the normalization of relative expression analysis for *SHISA7*. All samples were amplified in triplicates, and the relative expression data was analyzed according to the 2-ΔC t method, where ΔCt = Ct (*SHISA7*) – Ct (*G3PDH*). All the bar in the graphs were plotted as the mean ± SD.

The miRNA level cDNA samples in human, male and female Western chimpanzee, female crab-eating monkey, and male mouse were used with the HB_I Real-Time PCR Master mix kit (HeimBiotek) to perform qPCR, according to the manufacturer's protocol in a Rotor-Gene Q system, under the following qPCR conditions; initialization step at 95°C for 2 min, followed by 45 thermal cycles of 95°C for 5 s, 55°C for 10 s, and 72°C for 15 s; standard melting conditions of the ramp ranged from 55°C to 99°C, with a 1°C rise at each step. Small nuclear RNA (snRNA) U6 was used as the reference gene for normalization of relative expression analysis for miR-3681-5p (5′-UAGUGGAUGAUGCACUCUGUGC-3′). All samples were amplified in triplicates, and the relative expression data was analyzed according to the 2-ΔC t method, where ΔCt = Ct(hsa-miR-3681-5p) – Ct(U6). All the bar in the graphs were plotted as the mean ± SD.

Genomic DNA extraction and gene cloning

Genomic DNA was extracted from a human cell line HEK293A using DNeasy Blood & Tissue Kit (Qiagen), according to the manufacturer's protocol. Genomic DNA was then used for PCR amplification using the primer list shown in Table 2. The 20 μl PCR mix contained 10 μl of 2× TOPsimple DyeMix (aliquot)-HOT premix (Enzynomics, Korea), 7 μl of distilled water, 1 μl of gDNA template, and 1 μl of forward and reverse primers (10 pmole/μl) each. PCR conditions were as follows: initialization step at 95°C for 5 min, followed by 35 thermal cycles of 94°C for 40 s, annealing temperatures listed in Table 2 for 40 s, 72°C 40 s, and the final elongation step at 72°C 5 min. The PCR products were separated on a 1.5% agarose gel, and purified with Expin™ Gel SV (GeneAll), according to the manufacturer's protocol. The purified PCR products were cloned into a psi-CHECK2 vector (Promega, USA) using the LigaFast™ Rapid DNA Ligation System (Promega), as per the manufacturer's protocol. The cloned plasmid DNA was isolated by using Exprep™ Plasmid SV, mini (GeneAll).

Cell culture and luciferase assay

The lung cancer derived cell line A549 was grown at 37°C in a 5% (v/v) CO_2 incubator at Rosewell Park Memorial Institute (RPMI) (Gibco, USA), supplemented with 10% (v/v) heat-inactivated fetal bovine serum (FBS) (Gibco), and 1% (v/v) antibiotic-antimycotic (Gibco). The cells were plated in 24-well plates at a cell-density of 1×10^5 cells/well and grown to 80% confluence. After 24 h of incubation at 37°C in a 5% (v/v) CO_2 incubator, the cells were transfected with psi-CHECK2 vector cloned with different *SHISA7* regions and

miRNA mimics. A total of 500 ng of plasmid vector and 100 μM of mimics were used during cell transfection. Co-transfection was done using jetPRIME® (Polyplus, France), under the manufacturer's instructions. After 24 h of incubation at 37°C in a 5% (v/v) CO_2 incubator, the cells were lysed using 1× passive buffer (Promega), as per the manufacturer's protocol, followed by incubation in −80°C deep freezer for over 3 h. Firefly and Renilla luciferase activities were assessed using the Dual-Luciferase® Reporter Assay System (Promega), according to the manufacturer's instructions. Lane 1 was transfected with only the plasmid vector of each *SHISA7* region, lane 2 was co-transfected with plasmid vector containing miRNA negative control (Bioneer, Korea), lane 3 was co-transfected with plasmid vector containing miR-3681 mimic (Bioneer), lane 4 was co-transfected with plasmid vector containing miR-3681-5p inhibitor mimic (Bioneer), and lane 5 was co-transfected with plasmid vector containing both miR-3681 mimic and miR-3681-5p inhibitor mimic. The negative control mimic is made up of scrambled miRNAs; miR-3681 mimic is a chemically synthesized double-stranded RNA oligonucleotide and miR-3681-5p inhibitor is a single-stranded synthetic inhibitor with target miRNA complementary binding sequence. Each experiment was performed in triplicates and data is presented with bars as the mean ± SD. The Student's *t*-test in Excel 2016 (Microsoft, USA) was used to determine the significance of the results ($*P < 0.08$, $**P < 0.06$, $***P < 0.04$).

RESULTS

Long terminal repeats derived microRNA-3681

The sequence of hsa-miR-3681-5p (5′-UAGUGGAUGAUG-CACUCUGUGC-3′) was downloaded from miRbase v22.1 and used for blast search using the UCSC genome browser (GRCh38), to confirm the location and the nearest gene in human chromosomes. The seed region of hsa-miR-3681-5p is 5′-AGUGGAU-3′ and hsa-miR-3681 is present in the p arm of human chromosome 2. Moreover, hsa-miR-3681 overlaps with LTR16D1. The sequence of LTR16D1 was downloaded from the UCSC genome browser to determine the analogy between target miRNA and its derived gene (Fig. 1). The alignment result shows that hsa-miR-3681-5p is derived from LTR16D1, as seen from the perfectly matched sequence.

Bioinformatic analyses of hsa-miR-3681-5p and *SHISA7*

The target gene list of hsa-miR-3681-5p was downloaded from Target Scan Human and the candidates were selected based on the highest number of total seed sites that are complementary to the 3′ UTR of the target gene (Table 1). Out of 2,424 target genes, 13 were selected from the list and *SHISA7* showed the highest number of total seed sites and 8-mer hsa-miR-3681-5p binding sites in the 3′ UTR.

The schematic structure of *SHISA7* shows that it is inserted inversely in chromosome 19 of humans and that there are three CpG islands that cover the 5′ UTR, exon 2, and 3′ UTR, respectively (Fig. 2A). The CpG island on both UTRs are fully covered; however, the one on exon 2 is partially covered. The 3′ UTR of *SHISA7* contains a six 9-mer and two 8-mer hsa-miR-3681-5p complementary binding site (Supplementary Fig. S1). Using BiBiServ RNAhybrid, the structural interaction between hsa-miR-3681-5p and 3′ UTR of *SHISA7* was observed (Fig. 2B). The minimum free energy value between hsa-miR-3681-5p and *SHISA7* is −26.4 kcal/mol. The seed region of hsa-miR-3681-5p is well conserved when RNA hybrid with the 3′ UTR of *SHISA7*.

Three primers were designed from the 3′ UTR of *SHISA7* to examine if difference in expression is related to the number of 9-mer hsa-miR-3681-5p (Table 2). Primer #1, #2, and #3 have one, three, and six, 9-mer binding sites of hsa-miR-3681-5p in the 3′ UTR of *SHISA7,* respectively.

Relative expression analyses of hsa-miR-3681-5p and *SHISA7* in human, male and female Western chimpanzee, female crab-eating monkey, and male mouse tissues

Relative expression analyses of hsa-miR-3681-5p and *SHISA7*

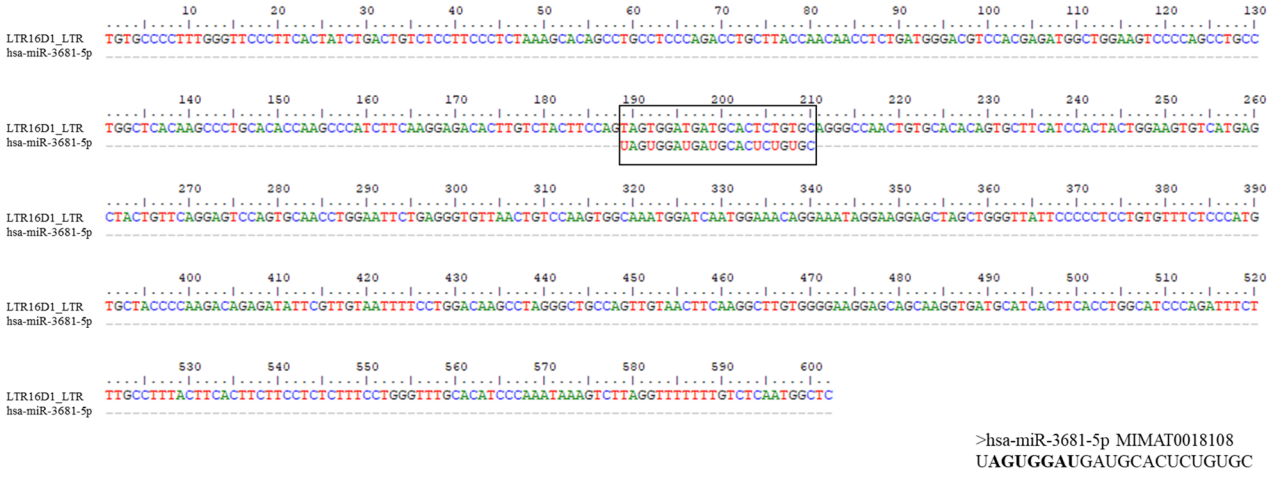

Fig. 1. The alignment result of LTR-LTR16D1 and hsa-miR-3681-5p. The black box shows the conserved region of hsa-miR-3681-5p and LTR16D1. The sequence of hsa-miR-3681-5p is shown under the alignment and the seed region is in bold.

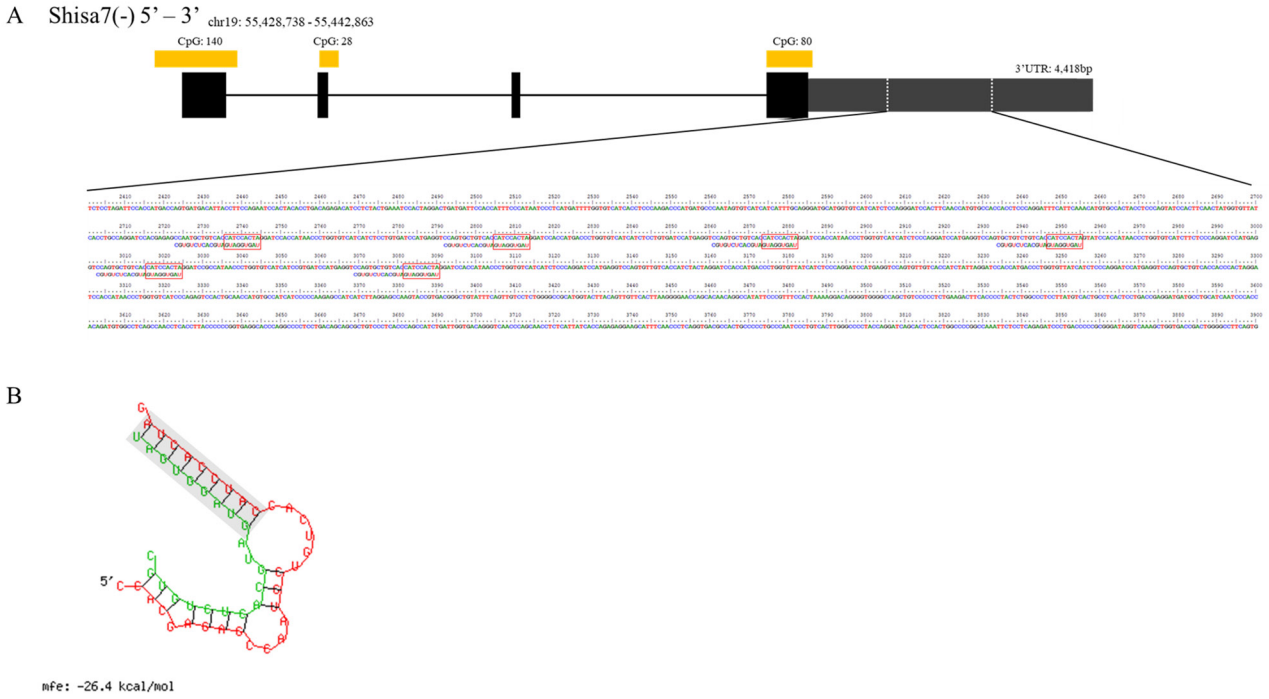

Fig. 2. Bioinformatics analysis of hsa-miR-3681-5p and its target gene *SHISA7*. (A) Schematic structure of *SHISA7* and the alignment result. The coding sequences are in black and the untranslated regions (UTRs) are in dark grey. Three CpG islands are present in *SHISA7*, and one each of the CpG island is covering the 5′ UTR, exon 2, and the 3′ UTR. CpG islands are shown in light grey. In the 3′ UTR of *SHISA7*, a total of six 9-mer binding sites of hsa-miR-3681-5p exist and from the sequence nine seeds of hsa-miR-3681-5p is shown in the black box. (B) RNA hybrid of hsa-miR-3681-5p and *SHISA7*. The seed region of hsa-miR-3681-5p and complementary binding site in the 3′ UTR of SHISA7 is shown in the grey box. The minimum free energy value between hsa-miR-3681-5p and 3′ UTR of *SHISA7* is -26.4 kcal/mol. The light green represents hsa-miR-3681-5p and red represents the 3' UTR of *SHISA7*.

was done by qPCR and re-analyzed using Heatmapper. The heatmap of relative expression of hsa-miR-3681-5p showed ubiquitous expression in human tissues; however, the values were under 0.004 (Fig. 3A). The muscles showed the highest, whereas the spleen and the lung the lowest, in humans. The male and female Western chimpanzees also showed low relative expression values of hsa-miR-3681-5p. For the male and female Western chimpanzees, the expression in the kidney and the small intestine was the highest (Figs. 3B and 3C), respectively. Interestingly, the female crab-eating monkeys showed high relative expression in the spinal cord with a value of over 0.12, whereas other tissues showed expression values lower than 0.02 (Fig. 3D). The heatmap of relative expression of hsa-miR-3681-5p in the male mice showed highest expression in the liver and the kidney; however, the value was between 0.0004 and 0.0005 (Fig. 3E). Lowest expression of hsa-miR-3681-5p was seen in the spleen of mice. A 9-mer hsa-miR-3681-5p binding site, in the 3′ UTR of *SHISA7*, showed expression in the stomach and the small intestine of humans; however, other tissues did not (Fig. 3A). The same 9-mer binding primer is relatively high in the testis, stomach, and cerebellum of the male Western chimpanzees (Fig. 3B), cerebellum of the female Western chimpanzees (Fig. 3C), and the bladder of the crab-eating monkeys (Fig. 3D). The male mice showed a higher expression value than hsa-miR-3681-5p, with the highest value of approximately 0.015 in the spleen and the lowest, approximately 0.002, in the kidney and the brain; both results being opposite, compared to hsa-miR-3681-5p (Fig. 3E). The three 9-mer hsa-miR-3681-5p binding site in the 3′ UTR of *SHISA7* showed highest relative expression in the brain of humans (Fig. 3A), the stomach and testis of the male Western chimpanzees (Fig. 3B), the cerebellum of the female Western chimpanzees (Fig. 3C), the bladder of the female crab-eating monkeys (Fig. 3D), and the spleen of the male mice (Fig. 3E). The three 9-mer binding sites in the 3′ UTR of *SHISA7* showed similar results to one 9-mer binding site in *SHISA7*; however, the expression value was greater in all samples.

Except for humans, the relative expression results for the female and male Western chimpanzees, crab-eating monkeys, and mice showed similar patterns for 9-mer hsa-miR-3681-5p binding sites. The male Western chimpanzees had the highest relative expression in the testis and the stomach for both one 9-mer hsa-miR-3681-5p binding primers (Fig. 3B). The female Western chimpanzees had the highest relative expression in the cerebellum for both 9-mer hsa-miR-3681-5p binding primers (Fig. 3C). The female crab-eating monkeys had the highest relative expression in the bladder for both primers (Fig. 3D). The male mice had the highest relative expression in the spleen and the lowest relative expres-

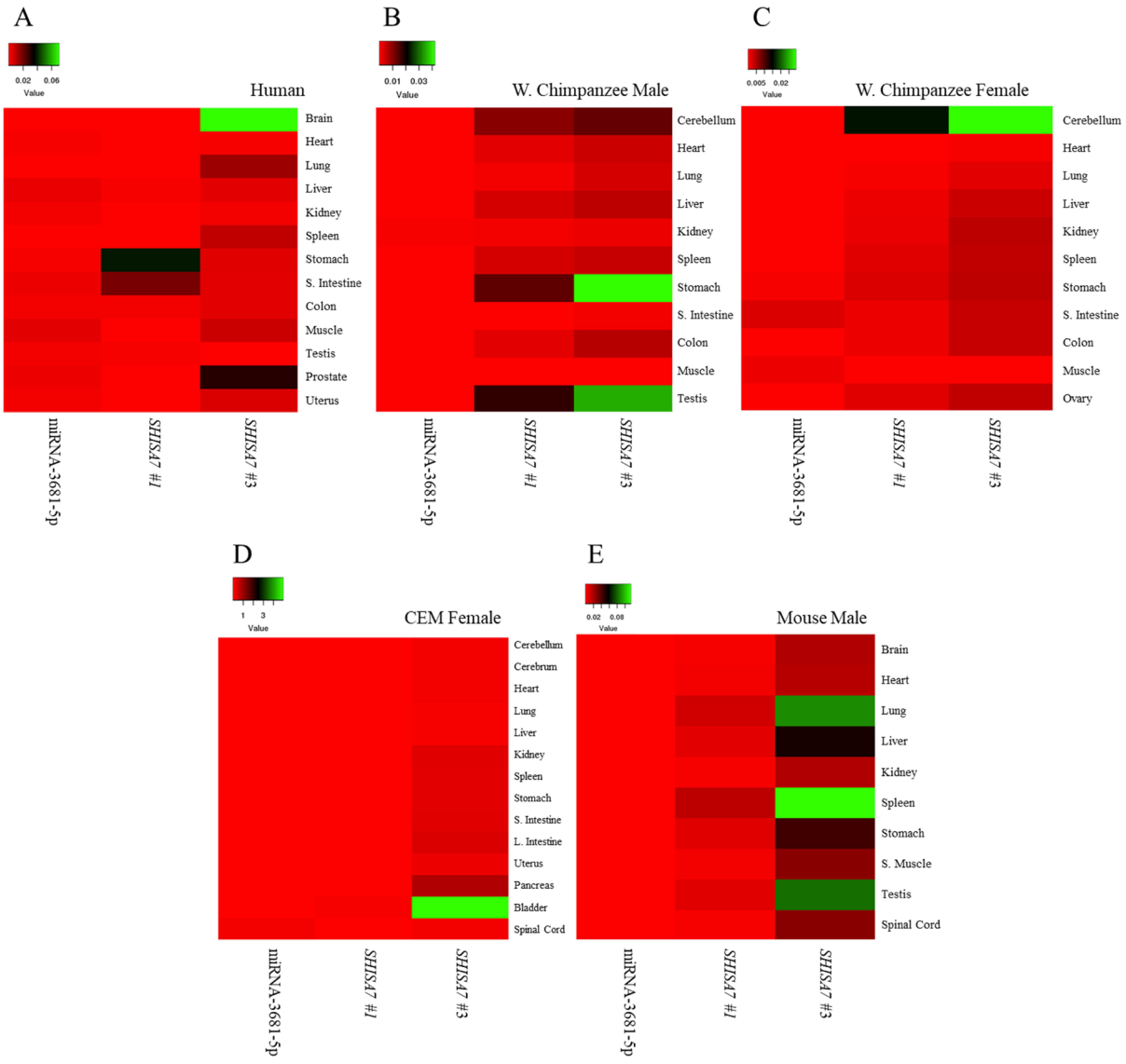

Fig. 3. Relative expression analyses of hsa-miR-3681-5p and *SHISA7* by heatmapper. (A) Heatmap of relative expression of hsa-miR-3681-5p and two primers of *SHISA7* in humans. (B) Heatmap of relative expression on hsa-miR-3681-5p and two primers of *SHISA7* in male Western chimpanzee. (C) Heatmap of relative expression on hsa-miR-3681-5p and two primers of *SHISA7* in female Western chimpanzee. (D) Heatmap of relative expression on hsa-miR-3681-5p and two primers of *SHISA7* in female crab-eating monkey. Crab-eating monkey is shortened as CEM. (E) Heatmap of relative expression on hsa-miR-3681-5p and two primers of *SHISA7* in male mouse.

sion in the kidney and the brain, for both primers (Fig. 3E). The relative expression data in graph of all hsa-miR-3681-5p and primers are shown in Supplementary Figs. S2-S6.

The luciferase analysis of hsa-miR-3681-5p and *SHISA7*

To analyze the correlation between the 3′ UTR of *SHISA7* and the number of 9-mer hsa-miR-3681-5p binding sites, the lung cancer derived cell line, A549, was used for co-transfection (Fig. 4). The result of one 9-mer for hsa-miR-3681-5p did not show any significant outcome. The result showed that, compared to control and the negative control, three and six 9-mer hsa-miR-3681-5p binding primers showed enhancer activity when hsa-miR-3681 mimic treatment was done. In contrast, the activity decreased when hsa-miR-3681-5p inhibitor was used. Interestingly, when the hsa-miR-3681 mimic and hsa-miR-3681-5p inhibitor are used together, the activity of three and six 9-mer hsa-miR-3681-5p binding plasmid enhanced approximately one and a half to two-fold more than when hsa-miR-3681 mimic was used alone.

The prediction of transcription factors in 3′ UTR of *SHISA7*

The 3′ UTR of *SHISA7* sequence was examined using TRANSFAC v8.0 with the assumption that the enhancer activity of *SHISA7*, with three and six 9-mer hsa-miR-3681, was in co-operation with TF. A total of 44 TF binding sites, with

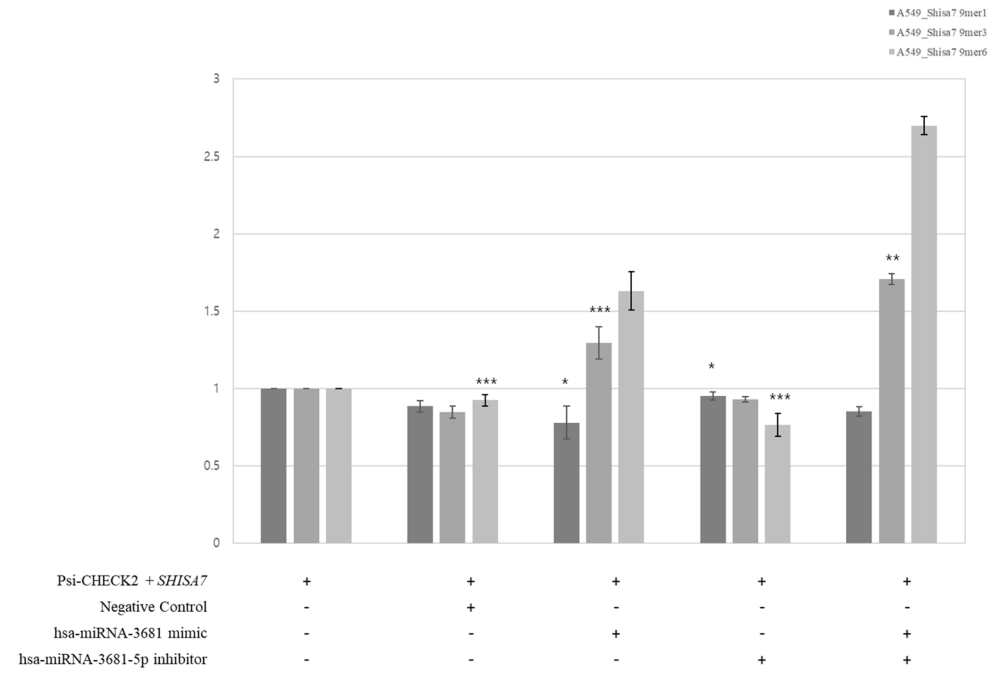

Fig. 4. Luciferase analysis of hsa-miR-3681-5p and *SHISA7* in A549 cell. The information on each color of the bar is provided at the top of the graph. All the bar in the graphs were plotted as the mean ± SD. The Student's *t*-test was used to determine the significance of the results. $*P < 0.08$, $**P < 0.06$, $***P < 0.04$.

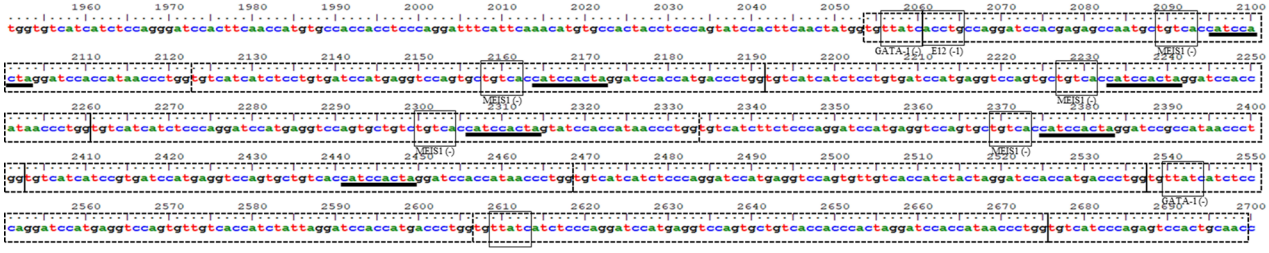

Fig. 5. Prediction of TF binding sites and VNTR in the 3′ UTR of *SHISA7*. Each predicted VNTR is divided with dotted boxes. The predicted TFs are in black boxes with the name of each TF and the 9-mer hsa-miR-3681-5p binding sites are in bold black lines.

thresholds of over 1 for core match and over 0.98 for matrix match, were found in the 3′ UTR of *SHISA7*.

The prediction and impact of VNTRs in the 3′ UTR of *SHISA7*

The sequence and name of the TFs near hsa-miR-3681-5p 9-mer seed regions are indicated within the box in Fig. 5. The prediction of TF provided the possibility of VNTR in the 3′ UTR of *SHISA7*.

The schematic structure of *SHISA7* and its sequence shows a detailed understanding of VNTRs in the 3′ UTR (Fig. 6A). The predicted VNTRs were aligned using BioEdit to determine the sequences (Fig. 6B). Interestingly, nine complete and one half of VNTR sequences were obtained near the 9-mer hsa-miR-3681-5p binding sites in the 3′ UTR of *SHISA7*. Six 9-mer hsa-miR-3681-5p binding sites were well conserved in VNTRs and except for a few unpaired sequences; approximately 70 to 75 sequences were present in the full VNTRs and approximately 25 to 30 nucleotides in the half VNTR.

DISCUSSION

This study focused on the idea that the number of miRNA binding sites in the 3′ UTR of a target gene will affect its expression. For evolutionary profiling, examination of the relative expression analysis on MDTE hsa-miR-3681-5p was performed by qPCR in the target gene of hsa-miR-3681-5p *SHISA7*, in human, chimpanzee, crab-eating monkey, and mouse. This analysis provided an understanding on how MDTE hsa-miR-3681-5p acted as an enhancer and blocked the activity of the VNTR.

SHISA7 is a well-known brain and neurotransmitter related gene; however, actual molecular biological studies on *SHISA7* are scarce (Cai et al., 2018; Han et al., 2019; Schmitz et al.,

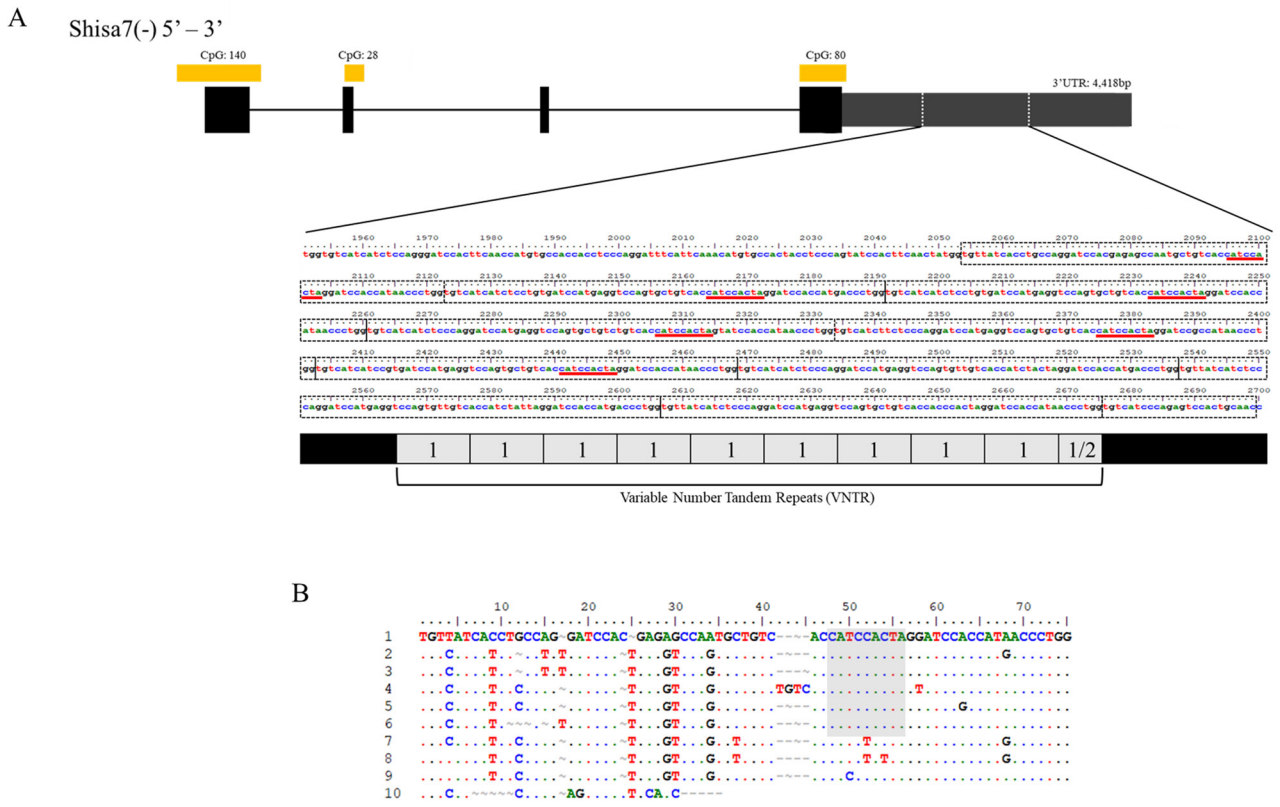

Fig. 6. Predicted VNTR regions in 3' UTR of *SHISA7*. (A) The schematic structure of VNTR in the 3′ UTR of *SHISA7*. The sequence of two white dotted lines, in the schematic structure of the 3′ UTR of *SHISA7*, is shown under the structure. Red bold lines represent the seed region of hsa-miR-3681-5p, and the dotted boxes in the sequence represent each VNTRs. Nine complete VNTRs and one half of VNTR sequences are seen. (B) The alignment of predicted VNTR in the 3′ UTR of *SHISA7*. A dot represents the identical nucleotide of the first sequence and a missing nucleotide is marked with a swung dash (~) or a hyphen (-). The grey box represents the conserved seed region of hsa-miR-3681-5p.

2017). Moreover, there is lack of studies on hsa-miR-3681-5p. Therefore, collecting data on hsa-miR-3681-5p and *SHISA7* has proven to be difficult. In our analysis, the heatmap showed that the relative expression value of hsa-miR-3681-5p was highest in the spinal cord of the crab-eating monkey and the value of hsa-miR-3681-5p was low in humans, chimpanzees, and mice (Fig. 3). The relative expression results with one and three 9-mer hsa-miR-3681-5p binding sites in the 3′ UTR of *SHISA7* showed an interesting pattern in chimpanzees, monkeys, and mice. The result from male and female chimpanzees, monkeys, and mice showed approximately two-fold higher expression value in the three 9-mer hsa-miR-3681-5p binding region than one 9-mer hsa-miR-3681-5p. The relative expression in humans did not show any distinguishing patterns; however, the expression of three 9-mer hsa-miR-3681-5p binding region in *SHISA7* increased greatly compared with one 9-mer hsa-miR-3681-5p binding primer. *SHISA7* is known as a brain related gene and human data shows that binding number of 9-mer hsa-miR-3681-5p is essential for relative expression. The product size of both primers was approximately 160 bp and the size of the primers did not affect the value of relative expression. Previously, *SHISA7* was shown to be a regulator of neurotransmitters and the species-based comparison of relative expression shows that humans and male and female chimpanzees have a similar pattern in the brain samples. The relative expression value was low in hsa-miR-3681-5p; however, the expression value for three hsa-miR-3681-5p binding region the in 3′ UTR of *SHISA7* was higher.

We hypothesized that the number of 9-mer hsa-miR-3681-5p binding sites affects the relative expression data and the luciferase assay. Previously, a miRNA study reported that miR-185 downregulates the expression of *SHISA7* in human and mouse neuroblastoma cells (Marques et al., 2012). In the case of hsa-miR-3681-5p, the plasmid with one of 9-mer hsa-miR-3681-5p binding site did not show any significant result; however, the plasmid with three and six 9-mer hsa-miR-3681-5p binding sites showed similar patterns. Instead of downregulating the *SHISA7*, the plasmid with three and six 9-mer hsa-miR-3681-5p binding regions up regulated the expression of *SHISA7*, in the presence of the hsa-miR-3681 mimic. In the presence of the hsa-miR-3681-5p inhibitor, the expression decreased more than the control. Interestingly, when both mimic and inhibitor were, the activity was upregulated, compared to the mimic treatment alone. The prediction was that since miRNA mimic is composed of

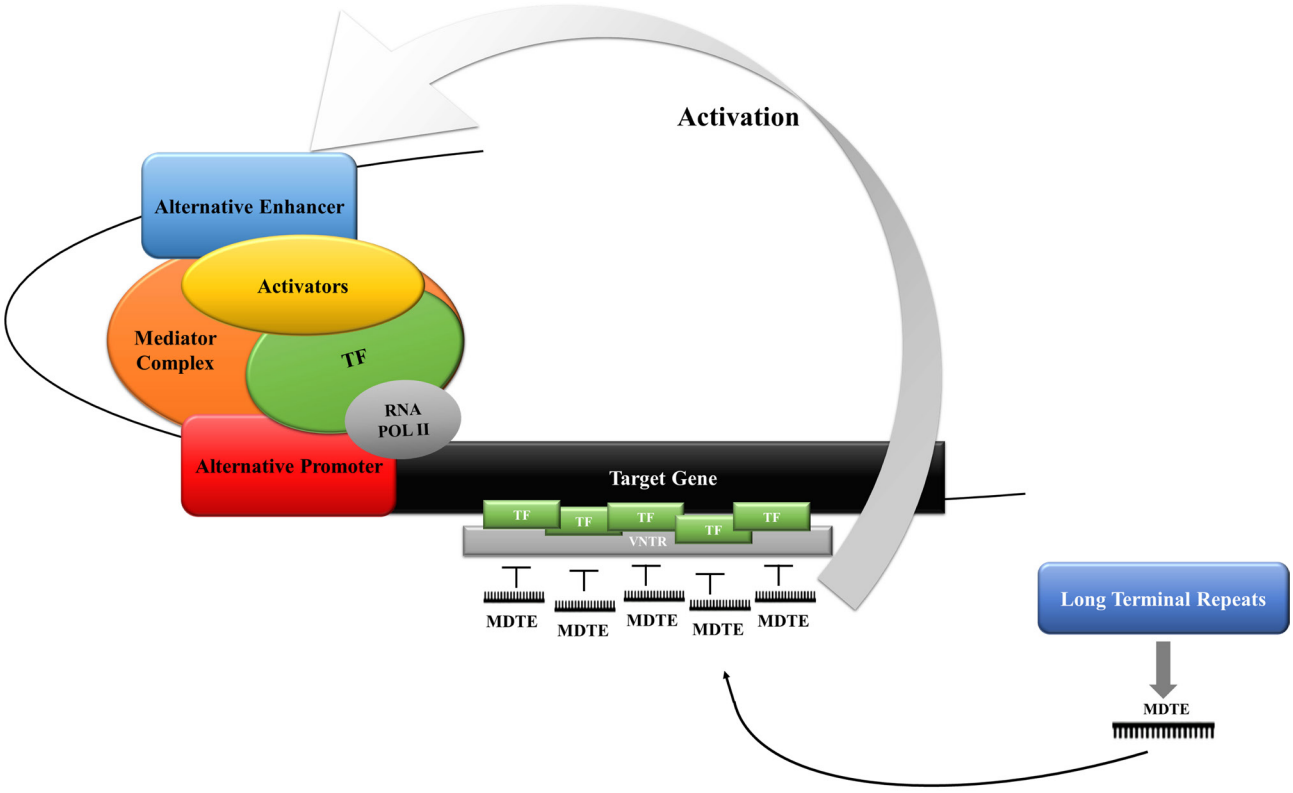

Fig. 7. Schematic illustration of overall summarization on enhancer activity of VNTR in 3' UTR of *SHISA7* repressed by hsa-miR-3681.

double-stranded RNA oligonucleotides of the target miRNA, hsa-miR-3681-3p must be affecting *SHISA7*, however, complementary binding sites for hsa-miR-3681-3p are not present in the 3′ UTR of *SHISA7*. To discover the enhancer activity in both the miRNA mimic and the inhibitor treated lane, the sequence of 3′ UTR *SHISA7* was analyzed and various TFs and VNTRs were seen to be included in the 3′ UTR of *SHISA7*. A total of nine and a half VNTRs existed and TFs in VNTR were present with their own patterns. TF MEIS1 was predicted near the seed region of five hsa-miR-3681-5p binding site and three TF GATA-1 was predicted near the 1st, 8th, and 9th VNTR start sites. The threshold of both core match and matrix match was set to 0.95 to check if there are missing GATA-1; however, TF prediction did not include more GATA-1. However, OF-miRNA-307 study provided the possibility that the TF near the binding site of miRNA in the 3′ UTR of the target gene might have a chance to cooperate with miRNA to gain enhancer activity (Lee et al., 2019).

Another diagnosis of enhancer activity shown in both hsa-miR-3681 mimic and hsa-miR-3681-5p inhibitor is VNTRs. VNTR and miRNA studies are scarce; however, a few studies have been done on brain disease related genes. A study analyzed autism and neurotransmitter related genes and miRNAs; MAOA, MAOB, DRD2, miRNA-431, and -21 for genomic sequence variations (Salem et al., 2013). Another study revealed that VNTRs regulate miRNA-137 by alternative splicing and this event increases the risk of schizophrenia (Pacheco et al., 2019). The deletion form of miRNA-137 transcripts is more frequent when an increased number of VNTRs were detected. Similar to our report, one of the reports used the luciferase assay to check VNTR and miRNA-491 expression (Jia et al., 2016). The result shows that when miRNA-491 mimic treatment was done with different number of VNTR copies, the expression was downregulated when more copies of VNTRs were included. In contrast, the expression was upregulated when anti-miRNA-491 was treated to different quantities of VNTR copies. In our report, the both hsa-miR-3681 mimic and hsa-miR-3681-5p inhibitor treatment result shows upregulation in all luciferase assays. The promoter activity is different within the length of VNTRs in the LTR12C element and it affects the expression of *RAE1* by cooperating with TF, NF-Y (Jung et al., 2017). The hypothesis was that miRNA affects VNTR by repressing the activity; in rare cases VNTRs gain enhancer activity by blocking hsa-miR-3681 mimics by hsa-miR-3681-5p inhibitor. In other words, we assume that VNTRs help hsa-miR-3681-5p to gain enhancer activity; however, the activity of VNTR might be repressed more than it should be by hsa-miR-3681-5p.

The illustration of the summary of this study can be seen in Fig. 7. miRNA derived from LTR or any of the TEs, called MDTEs, binds to the 3′ UTR of the target gene. In some cases, the 3′ UTR of target gene contains VNTRs such as *SHISA7* gene and this study provides the possibility that MDTE may enhances the gene expression, but its enhancer activity may represses the activity of VNTR. The MDTE recruits alternative enhancer and promoter, activators, mediators, TFs, and RNA

Pol II to function as an enhancer. The relative expression data confirmed that the number of miRNA binding sites is important for miRNA activity in the 3′ UTR of the target gene. Another evidence that miRNAs or MDTEs can function as enhancers is their ability to repress the activity of VNTRs. Further studies are needed to confirm that the enhancer activity of both hsa-miR-3681 mimic and hsa-miR-3681-5p inhibitor is contributed by VNTRs or TFs.

Note: Supplementary information is available on the Molecules and Cells website (www.molcells.org).

ACKNOWLEDGMENTS

This research was supported by the Cooperative Research Program of Primate Research Institute, Kyoto University (2019-B-7) and the National Research Foundation of Korea (NRF) funded by the Ministry of Education (NRF-2018R1D-1A1B07049460). We thank Kumamoto sanctuary and Primate Research Institute in Inuyama, Japan for providing the samples of Western chimpanzee male and female samples.

AUTHOR CONTRIBUTIONS

H.E.L. designed and performed all the experiments including writing the manuscript, J.W.H. and S.J.P. provided the crab-eating monkey samples, H.I. provided the Western chimpanzee samples, and H.S.K. commented and revised the manuscript.

CONFLICT OF INTEREST

The authors have no potential conflicts of interest to disclose.

ORCID

Hee-Eun Lee https://orcid.org/0000-0002-7485-9083
Sang-Je Park https://orcid.org/0000-0002-3371-9092
Jae-Won Huh https://orcid.org/0000-0001-5845-939X
Hiroo Imai https://orcid.org/0000-0003-0729-0322
Heui-Soo Kim https://orcid.org/0000-0002-5226-6594

REFERENCES

Agarwal, V., Bell, G.W., Nam, J.W., and Bartel, D.P. (2015). Predicting effective microRNA target sites in mammalian mRNAs. Elife *4*, e05005.

Agren, J.A. and Clark, A.G. (2018). Selfish genetic elements. PLoS Genet. *14*, e1007700.

Ambros, V., Bartel, B., Bartel, D.P., Burge, C.B., Carrington, J.C., Chen, X., Dreyfuss, G., Eddy, S.R., Griffiths-Jones, S., Marshall, M., et al. (2003). A uniform system for microRNA annotation. RNA *9*, 277-279.

Bartel, D.P. (2004). MicroRNAs: genomics, biogenesis, mechanism, and function. Cell *116*, 281-297.

Bourque, G., Burns, K.H., Gehring, M., Gorbunova, V., Seluanov, A., Hammell, M., Imbeault, M., Izsvak, Z., Levin, H.L., Macfarlan, T.S., et al. (2018). Ten things you should know about transposable elements. Genome Biol. *19*, 199.

Brummer, A. and Hausser, J. (2014). MicroRNA binding sites in the coding region of mRNAs: extending the repertoire of post-transcriptional gene regulation. Bioessays *36*, 617-626.

Cai, H., Zhu, X.X., Li, Z.F., Zhu, Y.P., and Lang, J.H. (2018). MicroRNA dysregulation and steroid hormone receptor expression in uterine tissues of rats with endometriosis during the implantation window. Chin. Med. J. (Engl). *131*, 2193-2204.

Feschotte, C. (2008). Transposable elements and the evolution of regulatory networks. Nat. Rev. Genet. *9*, 397-405.

Gonzalez-Cao, M., Iduma, P., Karachaliou, N., Santarpia, M., Blanco, J., and Rosell, R. (2016). Human endogenous retroviruses and cancer. Cancer Biol. Med. *13*, 483-488.

Gu, W., Xu, Y., Xie, X., Wang, T., Ko, J.H., and Zhou, T. (2014). The role of RNA structure at 5' untranslated region in microRNA-mediated gene regulation. RNA *20*, 1369-1375.

Hall, T.A. (1999). BioEdit: a user-friendly biological sequence alignment editor and analysis program for Windows 95/98/NT. Nucleic Acids Symp. Ser. *41*, 95-98.

Han, W., Li, J., Pelkey, K.A., Pandey, S., Chen, X., Wang, Y.X., Wu, K., Ge, L., Li, T., Castellano, D., et al. (2019). Shisa7 is a GABAA receptor auxiliary subunit controlling benzodiazepine actions. Science *366*, 246-250.

Hausser, J., Syed, A.P., Bilen, B., and Zavolan, M. (2013). Analysis of CDS-located miRNA target sites suggests that they can effectively inhibit translation. Genome Res. *23*, 604-615.

Hu, T., Pi, W., Zhu, X., Yu, M., Ha, H., Shi, H., Choi, J.H., and Tuan, D. (2017). Long non-coding RNAs transcribed by ERV-9 LTR retrotransposon act in cis to modulate long-range LTR enhancer function. Nucleic Acids Res. *45*, 4479-4492.

Inoue-Murayama, M., Adachi, S., Mishima, N., Mitani, H., Takenaka, O., Terao, K., Hayasaka, I., Ito, S., and Murayama, Y. (2002). Variation of variable number of tandem repeat sequences in the 3′-untranslated region of primate dopamine transporter genes that affects reporter gene expression. Neurosci. Lett. *334*, 206-210.

Jash, A., Yun, K., Sahoo, A., So, J.S., and Im, S.H. (2012). Looping mediated interaction between the promoter and 3' UTR regulates type II collagen expression in chondrocytes. PLoS One *7*, e40828.

Jia, X., Wang, F., Han, Y., Geng, X., Li, M., Shi, Y., Lu, L., and Chen, Y. (2016). miR-137 and miR-491 negatively regulate dopamine transporter expression and function in neural cells. Neurosci. Bull. *32*, 512-522.

Jung, Y.D., Lee, H.E., Jo, A., Hiroo, I., Cha, H.J., and Kim, H.S. (2017). Activity analysis of LTR12C as an effective regulatory element of the RAE1 gene. Gene *634*, 22-28.

Kel, A.E., Gossling, E., Reuter, I., Cheremushkin, E., Kel-Margoulis, O.V., and Wingender, E. (2003). MATCH: a tool for searching transcription factor binding sites in DNA sequences. Nucleic Acids Res. *31*, 3576-3579.

Kim, V.N. (2005). MicroRNA biogenesis: coordinated cropping and dicing. Nat. Rev. Mol. Cell Biol. *6*, 376-385.

Koressaar, T., Lepamets, M., Kaplinski, L., Raime, K., Andreson, R., and Remm, M. (2018). Primer3_masker: integrating masking of template sequence with primer design software. Bioinformatics *34*, 1937-1938.

Kozomara, A., Birgaoanu, M., and Griffiths-Jones, S. (2019). miRBase: from microRNA sequences to function. Nucleic Acids Res. *47*, D155-D162.

Lander, E.S., Linton, L.M., Birren, B., Nusbaum, C., Zody, M.C., Baldwin, J., Devon, K., Dewar, K., Doyle, M., FitzHugh, W., et al. (2001). Initial sequencing and analysis of the human genome. Nature *409*, 860-921.

Lee, H.E., Jo, A., Im, J., Cha, H.J., Kim, W.J., Kim, H.H., Kim, D.S., Kim, W., Yang, T.J., and Kim, H.S. (2019). Characterization of the long terminal repeat of the endogenous retrovirus-derived microRNAs in the olive flounder. Sci. Rep. *9*, 14007.

Lee, I., Ajay, S.S., Yook, J.I., Kim, H.S., Hong, S.H., Kim, N.H., Dhanasekaran, S.M., Chinnaiyan, A.M., and Athey, B.D. (2009). New class of microRNA targets containing simultaneous 5'-UTR and 3'-UTR interaction sites. Genome Res. *19*, 1175-1183.

Li, G., Wu, X., Qian, W., Cai, H., Sun, X., Zhang, W., Tan, S., Wu, Z., Qian, P., Ding, K., et al. (2016). CCAR1 5' UTR as a natural miRancer of miR-1254 overrides tamoxifen resistance. Cell Res. *26*, 655-673.

Liu, G., Zhang, R., Xu, J., Wu, C.I., and Lu, X. (2015). Functional conservation of both CDS- and 3'-UTR-located microRNA binding sites between

species. Mol. Biol. Evol. *32*, 623-628.

Marques, A.C., Tan, J., Lee, S., Kong, L., Heger, A., and Ponting, C.P. (2012). Evidence for conserved post-transcriptional roles of unitary pseudogenes and for frequent bifunctionality of mRNAs. Genome Biol. *13*, R102.

Nakamura, Y., Leppert, M., O'Connell, P., Wolff, R., Holm, T., Culver, M., Martin, C., Fujimoto, E., Hoff, M., Kumlin, E., et al. (1987). Variable number of tandem repeat (VNTR) markers for human gene mapping. Science *235*, 1616-1622.

O'Brien, J., Hayder, H., Zayed, Y., and Peng, C. (2018). Overview of microRNA biogenesis, mechanisms of actions, and circulation. Front. Endocrinol. (Lausanne) *9*, 402.

Pacheco, A., Berger, R., Freedman, R., and Law, A.J. (2019). A VNTR regulates miR-137 expression through novel alternative splicing and contributes to risk for schizophrenia. Sci. Rep. *9*, 11793.

Petri, R., Brattas, P.L., Sharma, Y., Jonsson, M.E., Pircs, K., Bengzon, J., and Jakobsson, J. (2019). LINE-2 transposable elements are a source of functional human microRNAs and target sites. PLoS Genet. *15*, e1008036.

Piriyapongsa, J. and Jordan, I.K. (2007). A family of human microRNA genes from miniature inverted-repeat transposable elements. PLoS One *2*, e203.

Piriyapongsa, J., Marino-Ramirez, L., and Jordan, I.K. (2007). Origin and evolution of human microRNAs from transposable elements. Genetics *176*, 1323-1337.

Qin, S., Jin, P., Zhou, X., Chen, L., and Ma, F. (2015). The role of transposable elements in the origin and evolution of microRNAs in human. PLoS One *10*, e0131365.

Rehmsmeier, M., Steffen, P., Hochsmann, M., and Giegerich, R. (2004). Fast and effective prediction of microRNA/target duplexes. RNA *10*, 1507-1517.

Roberts, J.T., Cardin, S.E., and Borchert, G.M. (2014). Burgeoning evidence indicates that microRNAs were initially formed from transposable element sequences. Mob. Genet. Elements *4*, e29255.

Sabino, F.C., Ribeiro, A.O., Tufik, S., Torres, L.B., Oliveira, J.A., Mello, L.E., Cavalcante, J.S., and Pedrazzoli, M. (2014). Evolutionary history of the PER3 variable number of tandem repeats (VNTR): idiosyncratic aspect of primate molecular circadian clock. PLoS One *9*, e107198.

Salem, A.M., Ismail, S., Zarouk, W.A., Abdul Baky, O., Sayed, A.A., Abd El-Hamid, S., and Salem, S. (2013). Genetic variants of neurotransmitter-related genes and miRNAs in Egyptian autistic patients. ScientificWorldJournal *2013*, 670621.

Schmitz, L.J.M., Klaassen, R.V., Ruiperez-Alonso, M., Zamri, A.E., Stroeder, J., Rao-Ruiz, P., Lodder, J.C., van der Loo, R.J., Mansvelder, H.D., Smit, A.B., et al. (2017). The AMPA receptor-associated protein Shisa7 regulates hippocampal synaptic function and contextual memory. Elife *6*, e24192.

Shi, F., Zhang, Y., Wang, J., Su, J., Liu, Z., and Wang, T. (2019). RNA-sequencing identified miR-3681 as a negative regulator in the proliferation and migration of cervical cancer cells via the posttranscriptional suppression of HGFR. RSC Adv. *9*, 22376-22383.

Thompson, P.J., Macfarlan, T.S., and Lorincz, M.C. (2016). Long terminal repeats: from parasitic elements to building blocks of the transcriptional regulatory repertoire. Mol. Cell *62*, 766-776.

Vaira, V., Roncoroni, L., Barisani, D., Gaudioso, G., Bosari, S., Bulfamante, G., Doneda, L., Conte, D., Tomba, C., Bardella, M.T., et al. (2014). microRNA profiles in coeliac patients distinguish different clinical phenotypes and are modulated by gliadin peptides in primary duodenal fibroblasts. Clin. Sci. (Lond). *126*, 417-423.

Vaz, C., Ahmad, H.M., Sharma, P., Gupta, R., Kumar, L., Kulshreshtha, R., and Bhattacharya, A. (2010). Analysis of microRNA transcriptome by deep sequencing of small RNA libraries of peripheral blood. BMC Genomics *11*, 288.

Wicker, T., Sabot, F., Hua-Van, A., Bennetzen, J.L., Capy, P., Chalhoub, B., Flavell, A., Leroy, P., Morgante, M., Panaud, O., et al. (2007). A unified classification system for eukaryotic transposable elements. Nat. Rev. Genet. *8*, 973-982.

Wingender, E., Chen, X., Fricke, E., Geffers, R., Hehl, R., Liebich, I., Krull, M., Matys, V., Michael, H., Ohnhauser, R., et al. (2001). The TRANSFAC system on gene expression regulation. Nucleic Acids Res. *29*, 281-283.

Yamamura, S., Imai-Sumida, M., Tanaka, Y., and Dahiya, R. (2018). Interaction and cross-talk between non-coding RNAs. Cell. Mol. Life Sci. *75*, 467-484.